


# Origin of isolated seamounts in the Canary Basin (East Atlantic): The role of plume material in the origin of seamounts not associated with hotspot tracks

Xiaojun Long<sup>1</sup>  | Jörg Geldmacher<sup>1</sup> | Kaj Hoernle<sup>1,2</sup> | Folkmar Hauff<sup>1</sup> | Jo-Anne Wartho<sup>1</sup> | C.-Dieter Garbe-Schönberg<sup>2</sup>

<sup>1</sup>GEOMAR Helmholtz Centre for Ocean Research Kiel, Kiel, Germany

<sup>2</sup>Institute of Geosciences, Kiel University, Kiel, Germany

## Correspondence

Xiaojun Long, GEOMAR Helmholtz Centre for Ocean Research Kiel, Wischhofstrasse 1-3, 24148 Kiel, Germany.  
Email: xlong@geomar.de

## Funding information

China Scholarship Council, Grant/Award Number: [2015]0672

## Abstract

In contrast to seamount chains, small solitary seamounts/seamount groups have rarely been sampled despite their large number and therefore their origins remain enigmatic. Here we present new <sup>40</sup>Ar/<sup>39</sup>Ar, trace element and Nd-Hf-Pb isotope data from the solitary Demenitskoy Seamount, the isolated Tolkien seamount group and the Krylov Seamount and Ridge in the Canary Basin, Central Atlantic Ocean. Their chemical compositions range from intraplate ocean-island-basalt (Demenitskoy) to mid-ocean-ridge-basalt (Tolkien and Krylov) types. Lavas from all three seamount groups, however, show geochemical evidence for involvement of enriched Canary/Cape Verde plume material. Seismic tomography shows that large areas around these mantle plumes consist of dispersed low-velocity material, which could represent diffusely-upwelling plume mantle. Melts from such upwelling mantle could form isolated seamounts. Diffuse upwelling of plume material is likely to be extremely widespread but has been poorly studied to date.

**Significance Statement:** A fundamental question concerns the origin of the hundreds of thousands of solitary seamounts and small isolated clusters of such seamounts on the seafloor of the world's ocean basins. Most of them do not fit into any currently accepted models (e.g. they are not associated with a linear hotspot track or plate boundary processes). Their formation could therefore represent a new kind of intraplate volcanism that in fact could be extremely widespread but has been thus far largely neglected. In this manuscript, we report geochemical data from three isolated seamount sites in the Canary Basin and propose a provocative model for their formation that can also be applied to isolated seamounts elsewhere. Our study is therefore also a plea for the long overdue systematic investigation of small seamount volcanism in the world's ocean basins.

I hereby confirm that all the data and interpretations are new and have not been published elsewhere. All co-authors have been actively involved in this work, have approved the manuscript and agreed to this submission.

This is an open access article under the terms of the Creative Commons Attribution-NonCommercial License, which permits use, distribution and reproduction in any medium, provided the original work is properly cited and is not used for commercial purposes.

© 2020 The Authors. *Terra Nova* published by John Wiley & Sons Ltd

## 1 | INTRODUCTION

Linear chains of intraplate volcanic islands and seamounts in the ocean basins are generally attributed either to mantle plumes (e.g. Morgan, 1971, 1972; Wilson, 1963) or to shallow tectonically driven processes (e.g. Hieronymus & Bercovici, 2000; Koppers, Staudigel, Pringle, & Wijbrans, 2003; Natland & Winterer, 2005). The earth's ocean floor, however, is dotted with hundreds of thousands of solitary seamounts/seamount clusters with heights of >1 km (Wessel, Sandwell, & Kim, 2010), which are not directly associated with age-progressive hotspot tracks and thus their origins remain enigmatic. In this study, we present  $^{40}\text{Ar}/^{39}\text{Ar}$  age, trace element and Nd-Hf-Pb isotope data of dredged rock samples from isolated seamounts at three locations in the Canary Basin (Figure 1). Their origin does not fit any currently accepted models and could represent a new kind of intraplate volcanism that in fact could be very common in the world's ocean basins but has not been extensively researched thus far.

## 2 | GEOLOGICAL BACKGROUND AND SAMPLING

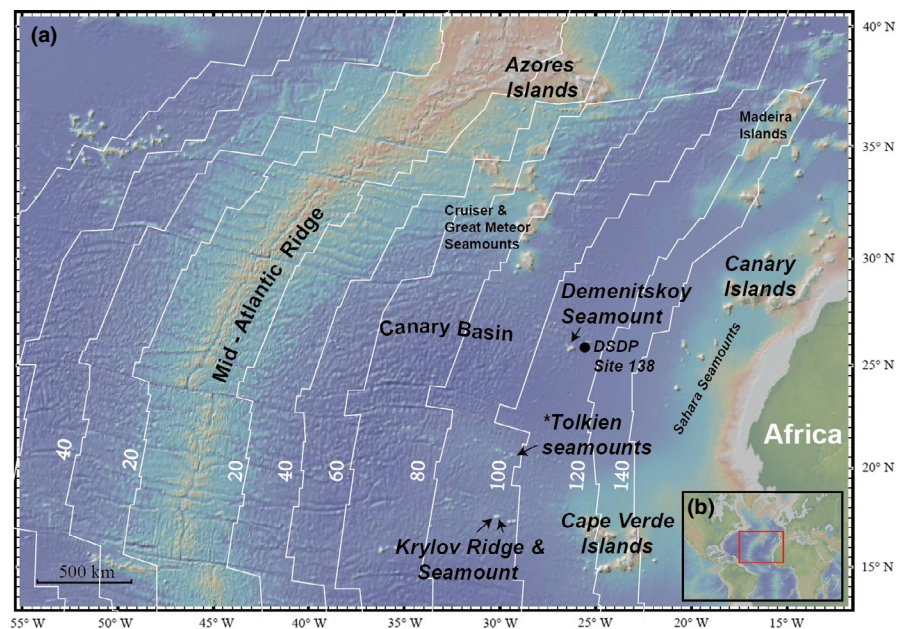
The Canary Basin in the central East Atlantic Ocean is bordered by the Canary Islands to the northeast, the Azores Archipelago to the northwest and the Cape Verde Islands to the southeast (Figure 1). Seismic tomography studies show that broad (up to 800 km across) low-velocity anomalies beneath the Canary, Cape Verde and Azores Islands can be traced into the deep mantle, where they coalesce (Montelli, Nolet, Dahlen, & Masters, 2006; Saki, Thomas, Nippres, & Lessing, 2015). Primitive (high)  $^3\text{He}/^4\text{He}$  ratios detected in phenocrysts of lavas from the Cape Verde Islands provide further support for the presence of lower mantle

material brought to the base of the lithosphere by a mantle plume (Doucelance, Escrig, Moreira, Gariépy, & Kurz, 2003), as does an age progression for the Canary Islands and associated seamounts to the northeast (Geldmacher, Hoernle, Bogaard, Duggen, & Werner, 2005).

The abyssal plain of the Canary Basin hosts several small and medium-sized isolated seamounts or small clusters of seamounts (Figure 1), which do not directly relate to any known hotspot tracks. The solitary Demenitskoy Seamount rises ~3,200 m from the sea floor and is located ~800 km to the southwest of the Canary Islands on ~110 Ma old oceanic crust (Müller et al., 2016). Bathymetric profiles indicate that Demenitskoy Seamount is a guyot (see Figure S1) and thus appears to have once formed an ocean island that was eroded to wave base. The Tolkien Seamount cluster consists of six unnamed seamounts located ~670 km southwest of Demenitskoy Seamount and ~750 km northwest of the Cape Verde Islands (Figure 1) on ~95 Ma old crust (Müller et al., 2016). The largest seamount "Tolkien" (Duggen, 2009) in the cluster rises to a height of ~2,750 metres-below-sea-level (m.b.s.l.). Krylov system is located ~300 km west of the Cape Verde Islands (Figure 1). Multi-beam mapping revealed a roundish ~960 m high cone, abutting a 15–20 km long E-W oriented ridge (Figure S1), that are named Krylov Seamount and Krylov Ridge respectively (Duggen, 2009). Krylov Ridge is oriented perpendicular to the MAR axis, subparallel to the prevailing strike of the fracture zones in the Canary Basin. The age of the oceanic crust beneath Krylov is ~95 Ma (Müller et al., 2016).

Since the ages and geochemical compositions of these seamounts are unknown, it is unclear if these volcanic edifices originally formed near the MAR, along fracture zones, or in an intraplate setting. During cruise POS397/1, volcanic rocks were dredged from the solitary Demenitskoy Seamount, the Tolkien Seamount cluster and the Krylov Seamount and Ridge (Duggen, 2009). Dredging information are summarized in Table S1.

**FIGURE 1** (a) Bathymetric map of the Canary Basin with the location of solitary seamounts and isolated small seamount clusters sampled for this study. \*Working name Tolkien was given to a nameless seamount by the POS379/1 scientific party (Duggen, 2009). White seafloor basement isochrons (in Ma) are based on Müller et al. (2016). Map created using GeoMapApp. The inset (b) shows the location of (a) within the central Atlantic Ocean. [Colour figure can be viewed at [wileyonlinelibrary.com](http://wileyonlinelibrary.com)]



### 3 | RESULTS

#### 3.1 | $^{40}\text{Ar}$ - $^{39}\text{Ar}$ age determinations

Only a single sample each from Demenitskoy and the Krylov seamounts were considered fresh enough to attempt age determination, but unfortunately neither of the samples yielded statistically valid plateau ages (Figure 2). Replicate analyses of sample DR5-1 from Demenitskoy Seamount yielded a complex age spectra and inverse isochrons that suggest  $^{39}\text{Ar}$  recoil, a problem commonly encountered in Cretaceous altered seafloor basalts (e.g., Koppers, Staudigel, & Wijbrans, 2000). Total fusion ages from the two splits were  $87.31 \pm 0.35$  and  $91.07 \pm 0.39$  Ma (all ages are quoted with  $2\sigma$  external uncertainties, unless otherwise stated), which are similar but do not overlap within errors. Applying the method of Fleck, Hagstrum, Calvert, Evarts, and Conrey (2014), 50% Ar recoil model ages were determined for these two replicated analyses, giving ages of  $86.8 \pm 2.8$  and  $89.6 \pm 3.6$  Ma (see Table S2 for more details). Combining these recoil model ages, we obtained an age of  $87.8 \pm 2.2$  Ma, which is the best age estimate for this Demenitskoy Seamount sample.

Replicate analyses of basaltic groundmass sample DR9-3 from Krylov Seamount yielded a similarly complex age spectra, with old low-temperature ages that were influenced by high levels of atmospheric Ar, and some suppression of the Ar isotope signals by high Cl levels. The old low-temperature ages may be due to either  $^{39}\text{Ar}$  recoil or excess  $^{40}\text{Ar}$ . The  $^{36}\text{Ar}/^{39}\text{Ar}$  Alteration Index (AI) values indicate the presence of fresh material for some of the high-temperature steps (Table S2) and the replicate analyses did yield overlapping high-temperature weighted mean (HT-WM) ages of  $68.46 \pm 0.69$  and

$69.55 \pm 0.76$  Ma (Figure 2) consistent with inverse isochron ages of  $68.54 \pm 0.69$  and  $62.4 \pm 7.8$  Ma. Combining the HT-WM ages from these two samples yielded a weighted mean age of  $69.02 \pm 0.56$  Ma ( $2\sigma$  uncertainties), which we interpret to be the best age estimate for this Krylov Seamount sample.

#### 3.2 | Trace element and isotopic variations

Thin section examination shows considerable submarine alteration. Therefore, we restrict this study to largely alteration-resistant immobile trace elements (Table S3) and to the Nd-Hf-Pb isotope systems (Table S4). A description of sample petrography, standard analytical methods and data quality information is given in the Supplemental Material.

Immobile trace element data are shown in Figures 3 and 4. Lavas from Demenitskoy Seamount show patterns with an overall enrichment of more over less incompatible elements and depletion in the heavy rare earth elements (HREE), characteristic of alkali ocean-island basalts (OIBs). The steep HREE patterns can be explained by the presence of residual garnet in the source. In contrast, Tolkien Seamount lavas display relatively flat patterns without significant HREE depletion, overlapping normal mid-ocean-ridge basalts (N-MORBs). Krylov Seamount and Ridge lavas, on the other hand, have intermediate, i.e., enriched (E-) MORB-type, compositions. Many lavas show an enrichment in Y relative to Dy and Ho coupled with a marked depletion in Ce indicating secondary alteration such as phosphatization (Hein et al., 2016). To assess this effect, we use the deviation of Y from HREEs with similar partition coefficients (Dy and Ho) as a filter ( $Y^* = (2 \times (Y)_n / ((Dy)_n + (Ho)_n))$ ). Only lavas with  $Y^*$

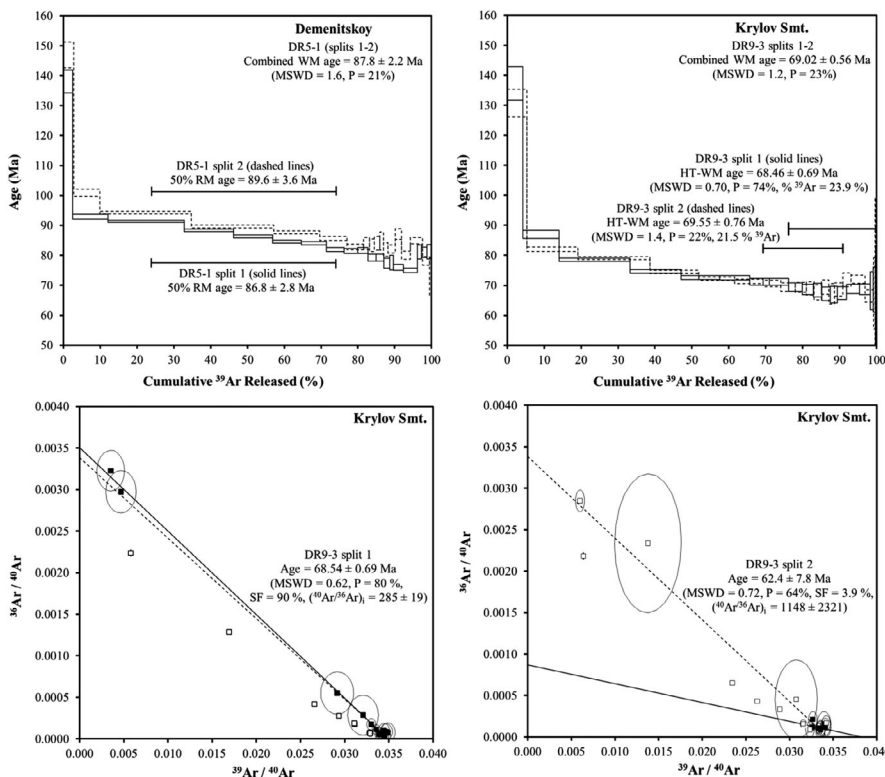


**FIGURE 2**  $^{40}\text{Ar}/^{39}\text{Ar}$  age spectra (top) and inverse isochron diagrams (bottom) of samples from Demenitskoy (DR5-1) and Krylov Seamounts (DR9-3). The black and white squares in the inverse isochron plots are selected high-temperature weighted mean and unselected analyses respectively. The solid line is the inverse isochron through the selected data, and the dashed line indicates an isochron line fit with an atmospheric  $^{40}\text{Ar}/^{36}\text{Ar}$  ratio. The age spectra y-axis box heights and the inverse isochron error ellipses correspond to  $2\sigma$  errors, and all ages are quoted with  $2\sigma$  external errors.

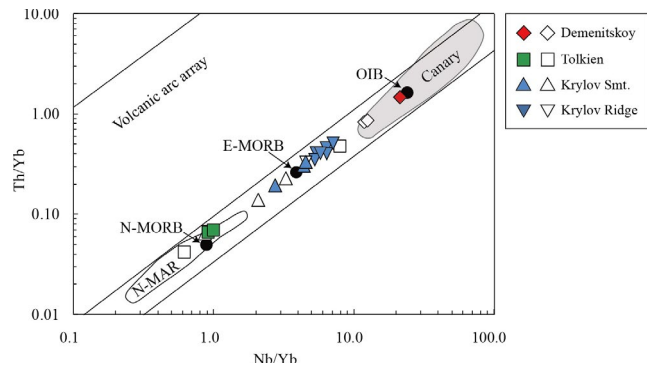


**FIGURE 3** FIGUREPlot of Nb/Yb versus Th/Yb ratios after (Pearce, 2008). In general, samples from Demenitskoy Seamount overlap with OIB compositions, whereas samples from Tolkien Seamount are similar to normal (N-) MORBs. Samples from Krylov Seamount and Ridge have transitional compositions and resemble enriched (E-) MORBs. The three black circles denote the average OIB, E-MORB and N-MORB compositions after Pearce (2008). Data for the Canary Island field were obtained from GEOROC (<http://georoc.mpch-mainz.gwdg.de/georoc/>), and the N-MAR MORB field data were acquired via PetDB Expert MORB (Mid-Ocean Ridge Basalt) Compilation after the compilation from Class, C. and Lehnert, K. (2012): <http://dx.doi.org/10.1594/IEDA/100060>. Relatively unaltered samples ( $Y^*$  values of  $1 \pm 0.1$ ) are shown with coloured (filled) symbols, whereas "more altered" samples are indicated by open symbols (see main text for details) [Colour figure can be viewed at [wileyonlinelibrary.com](http://wileyonlinelibrary.com)]

values of  $1 \pm 0.1$  are considered to be "relatively unaltered" and are shown with coloured (filled) symbols in Figures 3-5, whereas "more altered" samples are denoted by open symbols.

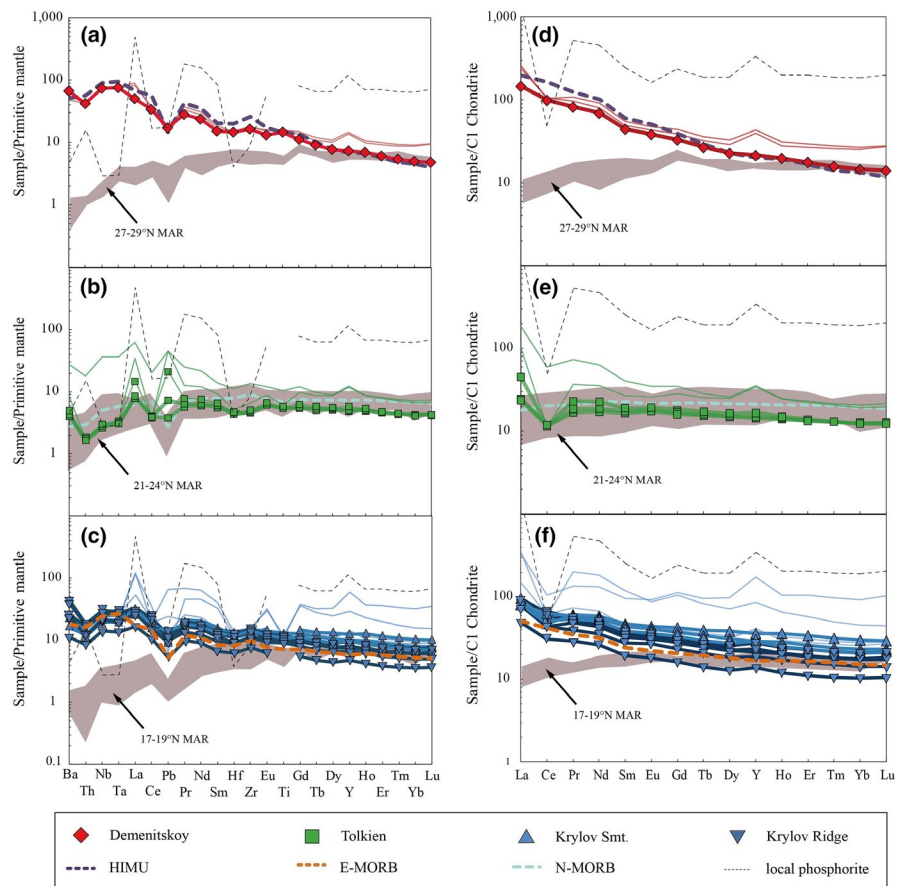
Ocean-island-basalt-like Demenitskoy lavas possess the most enriched Pb, Hf and Nd isotopic ratios (Figure 5), overlapping or plotting close to the compositional fields of the Canary and Cape Verde Islands (Figure 5). In contrast, Tolkien and Krylov Seamount lavas have less enriched Pb, Nd and Hf isotope ratios, overlapping or plotting close to the enriched end of the regional (16–30°N) present-day and late Mesozoic MORB composition. In summary, all seamount lavas plot between OIBs from the nearby Canary/Cape Verde Islands and the regional depleted upper mantle sampled by MORBs and thus could be derived from sources generated by mixing of these sources.

## 4 | DISCUSSION

### 4.1 | Origin of the seamounts

The age difference between the seamounts and the underlying oceanic crust can tell whether the seamounts were formed near a spreading ridge or in an intraplate setting. Subtracting the Demenitskoy Seamount  $^{40}\text{Ar}/^{39}\text{Ar}$  age of 88 Ma from the ~110 Ma old underlying lithospheric age (Müller et al., 2016), the lava erupted on ~22 Ma old crust, indicating an intraplate origin for this seamount consistent

**FIGURE 4** (a–c) Multi-element diagrams of fluid-immobile incompatible elements and (d–f) REEs, normalized to primitive mantle after Sun and McDonough (1989). Only lavas with  $Y^*$  values of  $1 \pm 0.1$  (see details in main text) are considered to be "relatively unaltered" and are shown with coloured symbols and thick lines, whereas the potentially altered samples are shown with thin lines, but without symbols. Grey fields indicate N-MORB compositions from mid-Atlantic ridge (MAR) segments at corresponding latitudes to the seamount locations. The thick purple, orange and green dashed lines indicate HIMU-type (high  $\mu$  = time-integrated  $^{238}\text{U}/^{204}\text{Pb}$ ) OIB (Willbold & Stracke, 2006), and E-MORB and N-MORB (Gale, Dalton, Langmuir, Su, & Schilling, 2013) compositions. [Colour figure can be viewed at [wileyonlinelibrary.com](http://wileyonlinelibrary.com)]



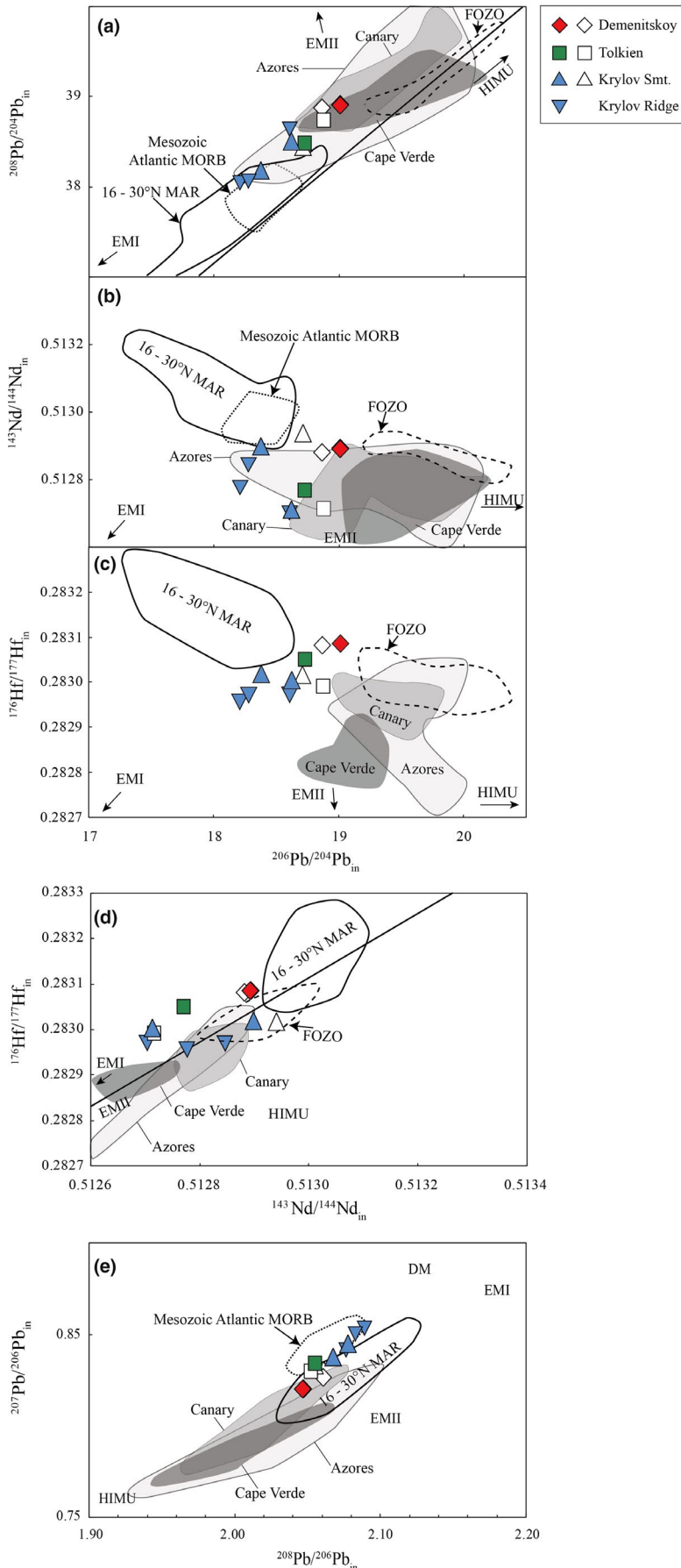


**FIGURE 5** Initial Nd-Pb-Hf isotope ratios of investigated seamount lavas shown in comparison to nearby MORB and OIB fields. Lavas that are potentially affected by secondary alteration (see main text for assessment) are shown with open symbols. Note that no significant difference in isotope compositions (all samples were acid-leached, see Supplemental Material) can be observed for potentially altered versus relatively unaltered lavas. The fields denoted by the black solid and black dashed lines indicate MORBs from the northern MAR (16–30°N; data were obtained from PetDB; <http://www.earthchem.org/petdb>) and central Atlantic Mesozoic ocean crust (with ages varying between 80 and 120 Ma from Janney and Castillo (2001)) respectively. Sources for Nd-Pb-Hf isotope data of lavas from the Canary, Cape Verde and Azores archipelagoes are listed in the Supplemental Material. For a better comparison, the present-day Canary, Cape Verde and Azores isotope data were corrected to 90 Ma for radiogenic ingrowth using the following assumed source parent and daughter element concentrations for Primitive Mantle ( $\text{Rb} = 0.635$ ,  $\text{Sr} = 21.100$ ,  $\text{Sm} = 0.444$ ,  $\text{Nd} = 1.354$ ,  $\text{U} = 0.021$ ,  $\text{Th} = 0.0850$ ,  $\text{Pb} = 0.1850$ ,  $\text{Lu} = 0.074$  and  $\text{Hf} = 0.309$ ; Sun & McDonough, 1989). The MORB data were also corrected to 90 Ma for radiogenic ingrowth using the Depleted Mantle (DM) parent and daughter element concentrations ( $\text{Rb} = 0.050$ ,  $\text{Sr} = 7.664$ ,  $\text{Sm} = 0.239$ ,  $\text{Nd} = 0.581$ ,  $\text{U} = 0.003$ ,  $\text{Th} = 0.008$ ,  $\text{Pb} = 0.018$ ,  $\text{Lu} = 0.058$  and  $\text{Hf} = 0.157$ ; Workman & Hart, 2005). Enriched mantle I and II (EMI and EMII) and HIMU isotope end member compositions are from Zindler and Hart (1986). [Colour figure can be viewed at [wileyonlinelibrary.com](http://wileyonlinelibrary.com)]

with its OIB-like incompatible-element composition. Oceanic crust of this age has a lithosphere thickness of ~50 km (Stein & Stein, 1992), restricting asthenospheric melting to this depth. The fractionated HREEs (Figure 4) either require initiation of melting in the garnet peridotite stability field at >70–80 km or derivation from garnet pyroxenite/eclogite, stable at depths of  $\geq 50$  km. Elevated temperature and deeper initiation of melting are consistent with a mantle plume source. In addition, the isotopic compositions of the Demenitskoy lavas are similar to those from the Canary/Cape Verde Islands, for which a mantle plume origin is generally accepted (e.g. French & Romanowicz, 2015; Hoernle, Tilton, & Schmincke, 1991; Montelli et al., 2006).

In contrast to Demenitskoy Seamount, the flat HREE patterns of the N-MORB-like lavas from Tolkien Seamount point to shallow melting predominately within the spinel stability field. In the absence of any radiometric age data, formation of the Tolkien Seamount at the MAR and subsequent passive drifting to its present position are therefore considered as the most likely origin for this seamount. Tolkien Seamount lavas show slightly enriched isotopic compositions plotting between the fields for Mesozoic MORBs and the Canary/Cape Verde plume lavas (Figure 5).

A limestone sample dredged during Russian cruise R/V Akademik N. Strakhov (1985) from the summit of Krylov Seamount (at 2,000 m.b.s.l.) contained an assemblage of Maestrichtian coccoliths (Il'in, 2000). A Maestrichtian (72.1–66.0 Ma; Cohen, Finney, Gibbard,

& Fan, 2019) minimum age for the underlying seamount volcanism is consistent with the combined high-temperature weighted mean  $^{40}\text{Ar}/^{39}\text{Ar}$  age of  $69.02 \pm 0.56$  Ma determined from a Krylov Seamount sample that was dredged from a similar depth. Therefore, the seamount must have formed on ~25 Ma old crust (at ~600 km distance from the spreading center) indicating an intraplate setting. The elongated sub-latitudinal orientation of the Krylov Seamount and Ridge on an extension of a fracture zone (Figure 1) suggests formation along a leaky fracture zone (Il'in, 2000), probably associated with local small-scale upwellings due to lithospheric extension. The E-MORB incompatible-element and slightly enriched (towards Canary/Cape Verde) isotopic compositions are consistent with the additional presence of plume-type mantle in the source. Waters, Sims, Perfit, Blichert-Toft, and Blusztajn (2011) have demonstrated that mixing of deeply generated pyroxenitic melts with shallowly generated spinel peridotite melts can generate E-MORB at fracture zones.

#### 4.2 | Common source material: Could non-hotspot-track seamounts also be derived from plume material?

The isotopic compositions of all investigated seamounts plot between enriched Canary/Cape Verde plume and depleted upper mantle compositions (late Mesozoic MORB), suggesting mixing

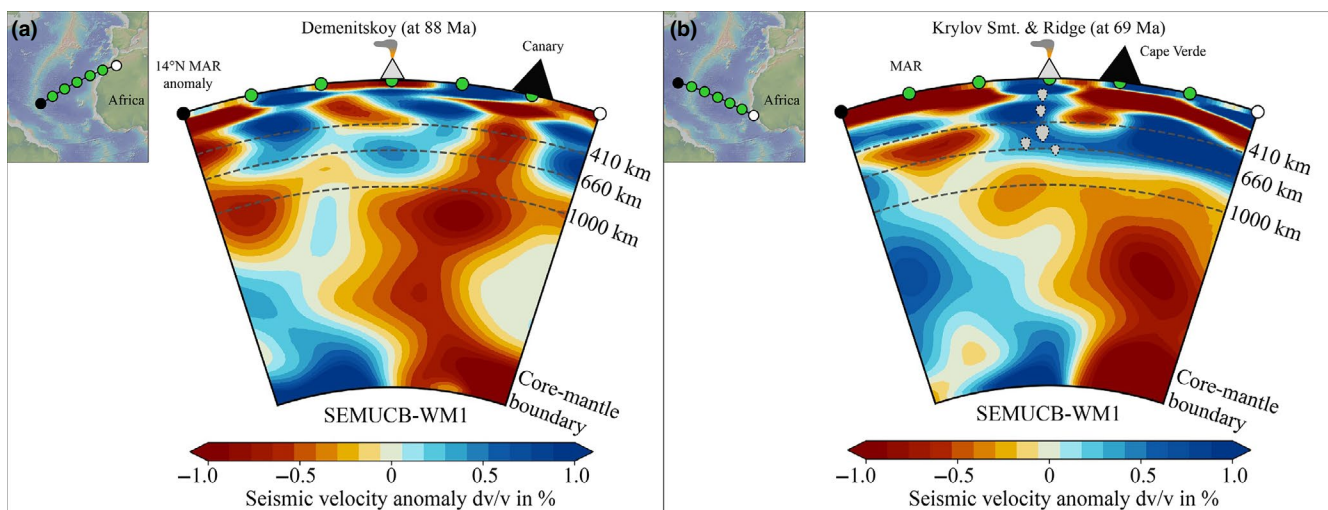


**FIGURE 6** Seismic tomographic cross sections of S-wave model SEMUCB-WM1 through the mantle beneath the East Atlantic (French & Romanowicz, 2015): (a) SW-NE striking profile running through the reconstructed site where Demenitskoy Seamount was emplaced ~88 Ma ago (modelled paleo-coordinates  $24.4^{\circ}\text{N}$ ,  $26.3^{\circ}\text{W}$ ) were calculated with Gplates software from Müller et al., 2016, and the rotation parameters of Matthews et al., 2016) and the present site of the Canary hotspot; (b) NW-SE profile through the site where the Krylov Seamount and Ridge were emplaced ~69 Ma ago ( $18.2^{\circ}\text{N}$ ,  $33.6^{\circ}\text{W}$ ) and the present location of the Cape Verde hotspot. In (a), there appears to be a continuous low-velocity anomaly extending from the base of the lower mantle to the base of the lithosphere beneath the Canary Islands, whereas Demenitskoy Seamount appears to be located above a series of large (>500 km wide and 100–300 km high) upwelling blobs. Small “plumelets” or blobs (added in grey) may have detached from the top of the anomalies ponded at ~1,000 km (Courtilot et al., 2003) and could have triggered transient intraplate volcanism (i.e. Demenitskoy, Krylov) and/or polluted the upper mantle feeding mid-ocean-ridge volcanism (Tolkien). Colour variations indicate faster (dark blue) or slower (dark red) velocities relative to the global average (light grey). Slower seismic velocities are generally interpreted to reflect hotter (or compositionally less dense) lithologies and their presence beneath most hotspots are believed to reflect conduits of upwelling plume material (e.g. Bijwaard & Spakman, 1999). It is unlikely that low-velocity (plume) material was only restricted to narrow conduits beneath the hotspots in the past but presumably showed similar distribution as shown in present-day tomographic models. [Colour figure can be viewed at [wileyonlinelibrary.com](http://wileyonlinelibrary.com)]

of plume mantle with depleted upper mantle (Figure 5). None of the seamounts, however, were formed closer than ~700 km to the nearest hotspot (using reconstruction parameters from Matthews et al., 2016 in GPlates software). Seismic tomographic models (e.g. French & Romanowicz, 2015; Montelli et al., 2006; Nolet, Allen, & Zhao, 2007), however, show that zones of slower seismic velocity are not restricted to narrow conduits beneath the respective active hotspots, but instead form large, irregularly-shaped zones in the lower mantle and isolated, discontinuous patches within the surrounding upper mantle (Figure 6a). Low-velocity anomalies beneath the Canary/Cape Verde hotspots appear to pond at mid-mantle depths at ~1,000 km below the spinel-perovskite plus magnesio-wüstite phase transition. This is an endothermic phase transition with a negative Clapeyron slope, impeding the passage of material (e.g. Cserepes & Yuen, 2000; Ito, Akaogi, Topor, & Navrotsky, 1990). In addition, upwelling plumes have to overcome a viscosity change at ~1,000 km (Rudolph, Lekić, & Lithgow-Bertelloni, 2015). Seismic tomography suggests that mantle pools and spreads out laterally at this depth (e.g. French & Romanowicz, 2015; Montelli et al., 2006). This phenomenon is also observed for low-velocity anomalies beneath many other hotspots (e.g. Hawaii, Iceland and St. Helena) and low-velocity anomalies that can be traced above this transition seem to shift laterally, branch out or appear to meander through the upper mantle (French & Romanowicz, 2015). Therefore, it appears that upwelling plume material pollutes large areas of the upper mantle around the main plume conduits (1,000 km or more from the active hotspots) and melting of this diffusely upwelling plume material could generate small isolated seamounts/seamount clusters.

It is also possible that small, secondary “plumelets” rise from the thermal boundary layer at the top of ponded, larger-scale anomalies (Courtillot, Davaille, Besse, & Stock, 2003). Such plumelets would be too small to be resolved by most global seismic tomographic models, but recently tomographic evidence has been found of several small upper-mantle upwellings (plumelets) rising several 100 km apart from each other through the transition zone below the northern East-African Rift system (Civiero, Armitage, Goes, & Hammond, 2019).

Slower seismic velocities are generally interpreted to reflect hotter or compositionally more fertile lithologies (e.g. Bijwaard & Spakman, 1999). Accordingly, upwelling hot and/or more fertile plume material would undergo decompression melting upon arrival at shallow mantle depths, regardless of whether the upwelling resulted from higher buoyancy of the plume material, small-scale upper mantle convection (e.g. Ballmer, van Hunen, Tackley, & Bianco, 2008), extension in the overriding ocean plate (e.g. along a fracture zone) or by upwelling related to seafloor spreading near a MOR. Melts from small isolated plumelets or from upwelling blobs of plume-type mantle would not create long-lasting hotspot tracks, although possibly form short clusters of volcanoes (Tolkien and Krylov) and isolated seamounts (Demenitskoy).

Many of the small, isolated seamounts that populate the ocean basins could potentially be related to such processes. Seamounts near the East Pacific Rise (5–15°N), for example, show enriched

isotopic compositions that are different from N-MORB (e.g., Graham et al., 1988; Niu, Regelous, Wendt, Batiza, & O'Hara, 2002). Other examples include the Pacific Pukapuka and Rano Rahi seamounts which show similar isotopic ranges (Hall, Mahoney, Sinton, & Duncan, 2006; Janney, Macdougall, Natland, & Lynch, 2000). The occurrence of isotopically enriched E-MORBs or OIBs far from any hotspot track attests to the ubiquitous presence of chemically enriched lithologies in the upper/mid mantle (e.g. Waters et al., 2011). In summary, our study suggests a common source for hotspot volcanoes and many of the isolated volcanic seamounts on the seafloor that are not directly related to age-progressive hotspot tracks. Clearly more studies of non-hotspot track seamounts are necessary to test the applicability of our model on a global scale.

#### ACKNOWLEDGEMENTS

The authors thank Captain M. Schneider, S. Duggen (chief scientist) and their crews on POS379/1 for obtaining the samples. The authors also thank S. Hauff, K. Junge, J. Sticklus (GEOMAR) and U. Westernströer (Kiel University) for the analytical support. Ingo Grevemeyer provided high-resolution bathymetric data (see Figure S1). J. Konter, G. Zhang and an anonymous reviewer are thanked for constructive reviews. The GEOMAR Helmholtz Center provided funding for analytical work, and the China Scholarship Council (CSC) for X.L.'s doctoral thesis.

#### DATA AVAILABILITY STATEMENT

The data that support the findings of this study are provided in the supplementary material.

#### ORCID

Xiaojun Long  <https://orcid.org/0000-0002-7331-7493>

#### REFERENCES

- Ballmer, M., van Hunen, J., Tackley, P., & Bianco, T. (2008). Non-hotspot volcano chains from small-scale sublithospheric convection (a 3D-numerical study). *Geophysical Research Abstracts* 10, EGU General Assembly (EGU2008-A-07167).
- Bijwaard, H., & Spakman, W. (1999). Tomographic evidence for a narrow whole mantle plume below Iceland. *Earth and Planetary Science Letters*, 166, 121–126. [https://doi.org/10.1016/S0012-821X\(99\)00004-7](https://doi.org/10.1016/S0012-821X(99)00004-7)
- Civiero, C., Armitage, J. J., Goes, S., & Hammond, J. O. (2019). The seismic signature of upper-mantle plumes: Application to the northern East African Rift. *Geochemistry, Geophysics, Geosystems*, 20(12), 6106–6122. <https://doi.org/10.1029/2019GC008636>
- Cohen, K. M., Finney, S. C., Gibbard, P. L., & Fan, J.-X. (2019). The International Commission on Stratigraphy international chronostratigraphic chart. *Episodes*, 36, 199–204.
- Courtillot, V. E., Davaille, A., Besse, J., & Stock, J. (2003). Three distinct types of hotspots in the Earth's mantle. *Earth Planet Science Letter*, 205, 295–308. [https://doi.org/10.1016/S0012-821X\(02\)01048-8](https://doi.org/10.1016/S0012-821X(02)01048-8)
- Cserepes, L., & Yuen, D. A. (2000). On the possibility of a second kind of mantle plume. *Earth and Planetary Science Letters*, 183, 61–71. [https://doi.org/10.1016/S0012-821X\(00\)00265-X](https://doi.org/10.1016/S0012-821X(00)00265-X)
- Doucelance, R., Escriú, S., Moreira, M., Gariépy, C., & Kurz, M. D. (2003). Pb-Sr-He isotope and trace element geochemistry of the Cape Verde Archipelago. *Geochimica et Cosmochimica Acta*, 67, 3717–3733. [https://doi.org/10.1016/S0016-7037\(03\)00161-3](https://doi.org/10.1016/S0016-7037(03)00161-3)

- Duggen, S. (2009). FS POSEIDON Fahrtbericht/Cruise Report P379/1: Vulkanismus im Karibik-Kanaren-Korridor (ViKKi). IFM-GEOMAR Report, 28, ISSN No: 1614-6298.
- Fleck, R. J., Hagstrum, J. T., Calvert, A. T., Evarts, R. C., & Conrey, R. M. (2014).  $^{40}\text{Ar}/^{39}\text{Ar}$  geochronology, paleomagnetism, and evolution of the Boring volcanic field, Oregon and Washington, USA. *Geosphere*, 10, 1283–1314. <https://doi.org/10.1130/GES00985.1>
- French, S. W., & Romanowicz, B. (2015). Broad plumes rooted at the base of the Earth's mantle beneath major hotspots. *Nature*, 525, 95–99. <https://doi.org/10.1038/nature14876>
- Gale, A., Dalton, C. A., Langmuir, C. H., Su, Y., & Schilling, J. G. (2013). The mean composition of ocean ridge basalts. *Geochemistry, Geophysics, Geosystems*, 14, 489–518. <https://doi.org/10.1029/2012GC004334>
- Geldmacher, J., Hoernle, K., Bogaard, P., Duggen, S., & Werner, R. (2005). New  $^{40}\text{Ar}/^{39}\text{Ar}$  age and geochemical data from seamounts in the Canary and Madeira volcanic provinces: Support for the mantle plume hypothesis. *Earth and Planetary Science Letters*, 237, 85–101. <https://doi.org/10.1016/j.epsl.2005.04.037>
- Graham, D. W., Zindler, A., Kurz, M. D., Jenkins, W. J., Batiza, R., & Staudigel, H. (1988). He, Pb, Sr and Nd isotope constraints on magma genesis and mantle heterogeneity beneath young Pacific seamounts. *Contributions to Mineralogy and Petrology*, 99, 446–463. <https://doi.org/10.1007/BF00371936>
- Hall, L. S., Mahoney, J. J., Sinton, J. M., & Duncan, R. A. (2006). Spatial and temporal distribution of a C-like asthenospheric component in the Rano Rahi Seamount Field, East Pacific Rise,  $15^{\circ}$ – $19^{\circ}$  S. *Geochemistry, Geophysics, Geosystems*, 7, 1–27. <https://doi.org/10.1029/2005GC000994>
- Hein, J., Koschinsky, A., Mikesell, M., Mizell, K., Glenn, C., & Wood, R. (2016). Marine phosphorites as potential resources for heavy rare earth elements and yttrium. *Minerals*, 6, 88. <https://doi.org/10.3390/min6030088>
- Hieronymus, C. F., & Bercovici, D. (2000). Non-hotspot formation of volcanic chains: Control of tectonic and flexural stresses on magma transport. *Earth and Planetary Science Letters*, 181, 539–554. [https://doi.org/10.1016/S0012-821X\(00\)00227-2](https://doi.org/10.1016/S0012-821X(00)00227-2)
- Hoernle, K., Tilton, G., & Schmincke, H.-U. (1991). Sr-Nd-Pb isotopic evolution of Gran Canaria: Evidence for shallow enriched mantle beneath the Canary Islands. *Earth and Planetary Science Letters*, 106, 44–63. [https://doi.org/10.1016/0012-821X\(91\)90062-M](https://doi.org/10.1016/0012-821X(91)90062-M)
- Il'in, A. (2000). On the origin and evolution of the Atlantis, Cruiser, Meteor, Rocket, and Krylov seamounts in the Atlantic Ocean. *Oceanology*, 40, 856–867.
- Ito, E., Akaogi, M., Topor, L., & Navrotsky, A. (1990). Negative pressure-temperature slopes for reactions forming  $\text{MgSiO}_3$  perovskite from calorimetry. *Science*, 249, 1275–1278. <https://doi.org/10.1126/science.249.4974.1275>
- Janney, P. E., & Castillo, P. R. (2001). Geochemistry of the oldest Atlantic oceanic crust suggests mantle plume involvement in the early history of the central Atlantic Ocean. *Earth and Planetary Science Letters*, 192, 291–302. [https://doi.org/10.1016/S0012-821X\(01\)00452-6](https://doi.org/10.1016/S0012-821X(01)00452-6)
- Janney, P. E., Macdougall, J. D., Natland, J. H., & Lynch, M. A. (2000). Geochemical evidence from the Pukapuka volcanic ridge system for a shallow enriched mantle domain beneath the South Pacific Superswell. *Earth and Planetary Science Letters*, 181, 47–60. [https://doi.org/10.1016/S0012-821X\(00\)00181-3](https://doi.org/10.1016/S0012-821X(00)00181-3)
- Koppers, A. A., Staudigel, H., Pringle, M. S., & Wijbrans, J. R. (2003). Short-lived and discontinuous intraplate volcanism in the South Pacific: Hot spots or extensional volcanism? *Geochemistry, Geophysics, Geosystems*, 4, 1–49. <https://doi.org/10.1029/2003GC000533>
- Koppers, A. A., Staudigel, H., & Wijbrans, J. R. (2000). Dating crystalline groundmass separates of altered Cretaceous seamount basalts by the  $^{40}\text{Ar}/^{39}\text{Ar}$  incremental heating technique. *Chemical Geology*, 166, 139–158. [https://doi.org/10.1016/S0009-2541\(99\)00188-6](https://doi.org/10.1016/S0009-2541(99)00188-6)
- Matthews, K. J., Maloney, K. T., Zahirovic, S., Williams, S. E., Seton, M., & Mueller, R. D. (2016). Global plate boundary evolution and kinematics since the late Paleozoic. *Global and Planetary Change*, 146, 226–250. <https://doi.org/10.1016/j.gloplacha.2016.10.002>
- Montelli, R., Nolet, G., Dahlen, F., & Masters, G. (2006). A catalogue of deep mantle plumes: New results from finite-frequency tomography. *Geochemistry, Geophysics, Geosystems*, 7, 1–69. <https://doi.org/10.1029/2006GC001248>
- Morgan, W. J. (1971). Convection plumes in the lower mantle. *Nature*, 230, 42–43. <https://doi.org/10.1038/230042a0>
- Morgan, W. J. (1972). Deep mantle convection plumes and plate motions. *AAPG Bulletin*, 56, 203–213. <https://doi.org/10.1306/819A3E50-16C5-11D7-8645000102C1865D>
- Müller, R. D., Seton, M., Zahirovic, S., Williams, S. E., Matthews, K. J., Wright, N. M., ... Cannon, J. (2016). Ocean basin evolution and global-scale plate reorganization events since Pangea breakup. *Annual Review of Earth and Planetary Sciences*, 44, 107–138. <https://doi.org/10.1146/annurev-earth-060115-012211>
- Natland, J. H., & Winterer, E. L. (2005). Fissure control on volcanic action in the Pacific. *Special Papers of the Geological Society of America*, 388, 687–688.
- Niu, Y., Regelous, M., Wendt, I. J., Batiza, R., & O'Hara, M. J. (2002). Geochemistry of near-EPR seamounts: Importance of source vs. process and the origin of enriched mantle component. *Earth and Planetary Science Letters*, 199, 327–345. [https://doi.org/10.1016/S0012-821X\(02\)00591-5](https://doi.org/10.1016/S0012-821X(02)00591-5)
- Nolet, G., Allen, R., & Zhao, D. (2007). Mantle plume tomography. *Chemical Geology*, 241, 248–263. <https://doi.org/10.1016/j.chemgeo.2007.01.022>
- Pearce, J. A. (2008). Geochemical fingerprinting of oceanic basalts with applications to ophiolite classification and the search for Archean oceanic crust. *Lithos*, 100, 14–48. <https://doi.org/10.1016/j.lithos.2007.06.016>
- Rudolph, M. L., Lekić, V., & Lithgow-Bertelloni, C. (2015). Viscosity jump in Earth's mid-mantle. *Science*, 350, 1349–1352. <https://doi.org/10.1126/science.aad1929>
- Saki, M., Thomas, C., Nippres, S. E., & Lessing, S. (2015). Topography of upper mantle seismic discontinuities beneath the North Atlantic: The Azores, Canary and Cape Verde plumes. *Earth and Planetary Science Letters*, 409, 193–202. <https://doi.org/10.1016/j.epsl.2014.10.052>
- Stein, C. A., & Stein, S. (1992). A model for the global variation in oceanic depth and heat flow with lithospheric age. *Nature*, 359, 123–129. <https://doi.org/10.1038/359123a0>
- Sun, S.-S., & McDonough, W.-S. (1989). Chemical and isotopic systematics of oceanic basalts: Implications for mantle composition and processes. *Geological Society, London, Special Publications*, 42, 313–345. <https://doi.org/10.1144/GSL.SP.1989.042.01.19>
- Waters, C. L., Sims, K. W., Perfit, M. R., Blichert-Toft, J., & Blusztajn, J. (2011). Perspective on the genesis of E-MORB from chemical and isotopic heterogeneity at  $9$ – $10^{\circ}$  N East Pacific Rise. *Journal of Petrology*, 52, 565–602. <https://doi.org/10.1093/petrology/egq091>
- Wessel, P., Sandwell, D. T., & Kim, S. S. (2010). The global seamount census. *Oceanography*, 23, 24–33. <https://doi.org/10.5670/oceanog.2010.60>
- Willbold, M., & Stracke, A. (2006). Trace element composition of mantle end-members: Implications for recycling of oceanic and upper and lower continental crust. *Geochemistry, Geophysics, Geosystems*, 7, 1–30. <https://doi.org/10.1029/2005GC001005>
- Wilson, J. T. (1963). A possible origin of the Hawaiian Islands. *Canadian Journal of Physics*, 41, 863–870. <https://doi.org/10.1139/p63-094>



- Workman, R. K., & Hart, S. R. (2005). Major and trace element composition of the depleted MORB mantle (DMM). *Earth and Planetary Science Letters*, 231, 53–72. <https://doi.org/10.1016/j.epsl.2004.12.005>
- Zindler, A., & Hart, S. (1986). Chemical geodynamics. *Annual Review of Earth and Planetary Sciences*, 14, 493–571. <https://doi.org/10.1146/annurev.ea.14.050186.002425>

#### SUPPORTING INFORMATION

Additional supporting information may be found online in the Supporting Information section.

**Figure S1.** Bathymetric maps of investigated isolated seamounts/seamount clusters.

**Table S1.** Sampling sites.

**Table S2.** Demenitskoy and Krylov Seamounts  $^{40}\text{Ar}/^{39}\text{Ar}$  basaltic

groundmass ages.

**Table S3.** Trace element concentrations.<sup>a</sup>

**Table S4.** Nd-Pb-Hf isotope ratios.\*

**Supplementary Material.** Analytical methods and citations of reference fields in Figure 5.

**How to cite this article:** Long X, Geldmacher J, Hoernle K, Hauff F, Wartho J-A, Garbe-Schönberg C-D. Origin of isolated seamounts in the Canary Basin (East Atlantic): The role of plume material in the origin of seamounts not associated with hotspot tracks. *Terra Nova*. 2020;32:390–398. <https://doi.org/10.1111/ter.12468>